PHYSICAL REVIEW B **84**, 220104(R) (2011)

Ground-state structures of ice at high pressures from *ab initio* random structure searching

Jeffrey M. McMahon[*]
Department of Physics, University of Illinois at Urbana-Champaign, Illinois 61801, USA

(Received 9 June 2011; revised manuscript received 5 October 2011; published 13 December 2011)

Ab initio random structure searching based on density functional theory is used to determine the ground-state structures of ice at high pressures. Including estimates of lattice zero-point energies, ice is predicted to adopt at least three crystal phases beyond $Pbcm$. The underlying sublattice of O atoms remains similar among them, and the transitions can be characterized by reorganizations of the hydrogen bonds. The symmetric hydrogen bonds of ice X and $Pbcm$ are initially lost as ice transforms to structures with symmetries $Pmc2_1$ (800–950 GPa) and $P2_1$ (1.17 TPa), but they are eventually regained at 5.62 TPa in a layered structure $C2/m$. The $P2_1 \rightarrow C2/m$ transformation also marks the insulator-to-metal transition in ice, which occurs at a significantly higher pressure than recently predicted.

DOI: 10.1103/PhysRevB.84.220104 PACS number(s): 64.70.K−, 62.50.−p, 71.30.+h, 96.15.Nd

The behavior of H_2O at high pressures is of fundamental importance for both condensed-matter and planetary physics.[1,2] This can be attributed to its substantial abundance in the universe, and the fact that a significant fraction of it exists in ice form at high pressures in planetary interiors. In our solar system alone, for example, Uranus and Neptune consist largely of H_2O, ammonia, and methane ice mixtures up to 800 GPa, and the cores of Saturn and Jupiter likely contain ice components (but perhaps liquid, due to extreme temperatures—see below) at pressures of ∼800 GPa–1.8 TPa and 4–5 TPa, respectively.[3] Despite this importance, very little is known about the behavior of solid H_2O (ice) under these extreme conditions. This is because static-compression experiments have thus far only reached 210 GPa.[4] Shock compression can achieve greater pressures, but only at significantly higher temperatures.[5] However, ramp-wave compression techniques are expected to achieve TPa pressures at comparatively low temperatures in the near future.[6] Furthermore, until recently, theoretical and computational methods have not existed to reliably predict crystal structures with little to no *a priori* information.

The phase diagram of H_2O is already extremely rich. To date, ten thermodynamically stable and six metastable phases are known,[7] ice XV being discovered only recently.[8] The highest-pressure phase experimentally observed is ice X, which is obtained from a phase transition from ice VII (or VIII, depending on the temperature) near 44 GPa.[9] In this phase, the O atoms form a body-centered-cubic (bcc) sublattice and the H atoms adopt symmetric positions between them at pressures near 110–120 GPa.[10] Because of this, the distinction between covalent bonds and hydrogen bonds is lost, as is thus the molecular form of H_2O, resulting in an atomic solid. Recent lattice dynamics calculations using density functional theory (DFT) suggest that the symmetric ordered form of ice X is only stable from 120 to 400 GPa.[11] Near 300–400 GPa, a lattice instability occurs, resulting in a transition to a crystal phase with $Pbcm$ symmetry (Hermann-Mauguin space-group symbol), where the O atoms adopt a distorted hexagonal close-packed (hcp) configuration,[11] as predicted by Benoit *et al.* in 1996 via a constant pressure molecular dynamics simulation.[12] At even higher pressures, which is of fundamental importance to planetary physics, for example, very little is known. However, a number of intriguing possibilities have been proposed, perhaps the most interesting being an insulator-to-metal transition.[13,14]

In this Rapid Communication, the recently proposed *ab initio* random structure searching (AIRSS) method of Pickard and Needs to predict crystal structures,[15] combined with DFT, is used to determine the ground-state structures of ice at high pressures. In this method, a number of random configurations are each relaxed at constant pressure. After enough trials, a good sampling of the configuration space is obtained, and the ground-state structure(s) can be identified. This method has been used to successfully predict the ground-state structures of a number of systems,[16] recently including those of atomic metallic hydrogen, for example.[17]

Calculations were performed using the Quantum ESPRESSO (QE) DFT code.[18] Norm-conserving Troullier-Martins pseudopotentials[19] were used for all calculations. For O, a He-core pseudopotential with valence core radii of 1.25, 1.25, and 1.4 a.u. for the s, p, and d components, respectively, was used.[20] For H, a core radius of 0.8 a.u. was used for the AIRSS and then decreased to 0.3 a.u. for recalculating detailed enthalpy versus pressure curves. For all calculations, the Perdew-Burke-Ernzerhof generalized gradient approximation (GGA) exchange and correlation functional[21] was used. See Ref. 22 for justifications for these approximations, as well as Ref. 23 for a discussion of the necessary use of GGA to describe hydrogen bonding. A plane-wave basis set with a cutoff of ∼1633 eV was used for the AIRSS and then increased to ∼4762 eV for recalculating enthalpy curves. For Brillouin-zone (BZ) sampling, 8^3 **k** points were used for all calculations, except for $Cmcm$, $Cmca$, $P4_2/nnm$, and $P2_1/m$ (see below) for which 12^3 were used when recalculating enthalpy curves. The cutoff and **k**-point sampling were found to give a total convergence in energy to better than ∼0.01 eV/H_2O and the total pressure to ∼1 GPa for each structure. Phonons were calculated using density functional perturbation theory as implemented within QE, and were converged to a similar level of accuracy as the DFT calculations. Electronic band-gaps were calculated using the tetrahedron method.[24]

Random structures were constructed by generating random unit-cell translation vectors, renormalizing the volume, and choosing random H_2O configurations (positions and

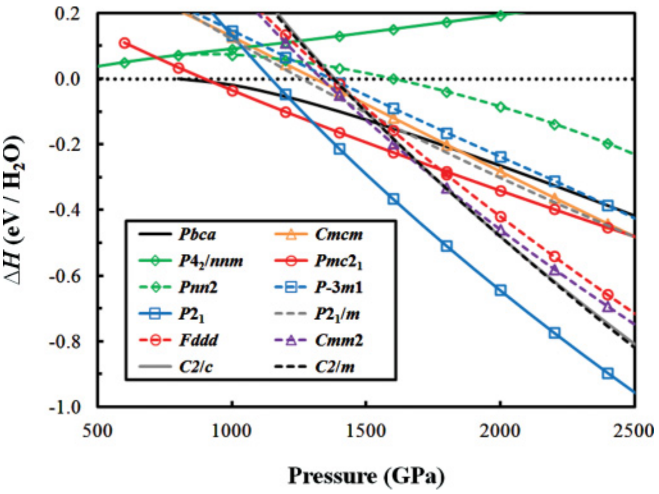

FIG. 1. (Color online) Enthalpies of the ground-state structures of ice relative to *Pbcm* (shown as a dotted line), not including lattice zero-point energies. Note that the enthalpies versus pressure are nearly linear from 2.5 to 5 TPa (not shown).

orientations). Constant pressure geometry relaxations were then performed at 0.5, 1, 1.5, 2, 3, and 5 TPa for unit cells containing four H_2O units, and then additional relaxations were performed at 1 and 2 TPa using unit cells containing six and eight H_2O units. (However, the latter searches only revealed a couple of additional structures—see below and Ref. 22.) It is important to realize that searches over factorized unit-cells are implicitly included in these calculations—i.e., those with one, two, or three H_2O units. While structures with unit cells containing other numbers of H_2O units are certainly possible, it is reasonable to suspect that they are unlikely based on comparisons with the other predicted high-pressure phases of ice, such as *Pbcm* (Ref. 12) and the recently proposed *Cmcm* and *Pbca* structures[14] (all found via simulations capable of generating unit cells with up to 16 H_2O units). Typical relaxations included up to 175 random structures at each pressure considered, which appeared to be enough to generate both the lowest-enthalpy structure and higher-enthalpy metastable ones multiple times. See Ref. 22 for a justification of this methodology, as well as support for the predicted ice X → *Pbcm* transformation.[12]

After performing the AIRSS, each structure within ~0.35 eV/H_2O of the lowest-enthalpy one found was considered for further investigation. Detailed enthalpy versus pressure curves were calculated for these structures by performing additional constant-pressure geometry optimizations while keeping symmetries fixed; see Fig. 1. Note that a discussion of the metastable structures not explicitly considered below can be found in Ref. 22. (Also note that discussions of the metastable structures and related AIRSS at lower pressures can be found in Refs. 25 and 26, respectively.)

Near 800 GPa, *Pbcm* becomes unstable relative to two additional structures, $Pmc2_1$ and *Pbca*. Such instability is expected, as it has been demonstrated that *Pbcm* develops a dynamic instability near 760 GPa in the (1/2,0,0) phonon mode.[14] Both *Pbcm* and $Pmc2_1$ are shown in Fig. 2, and *Pbca* is shown in Refs. 14 and 22. $Pmc2_1$ and *Pbca* are both similar to *Pbcm*. For example, in the perspective of Fig. 2, the O atoms remain close to their distorted hcp-sublattice positions.[12] However, the H atoms are shifted away from their symmetric O-H-O positions. In *Pbca*, a small distortion of the H atoms occurs in alternating directions, leaving them close to tetrahedral sites and the hydrogen-bond network intact. In $Pmc2_1$, on the other hand, a reorganization of the hydrogen-bond network occurs. In the perspective of Fig. 2, every O atom in *Pbcm* is connected to both its vertical and horizontal neighbors via symmetric hydrogen bonds. In $Pmc2_1$, this bonding is only retained in every other column of O atoms, but without symmetric hydrogen bonds. The other O atoms become disconnected from their vertical neighbors, and instead become unsymmetrically hydrogen bonded with O atoms out of the plane.

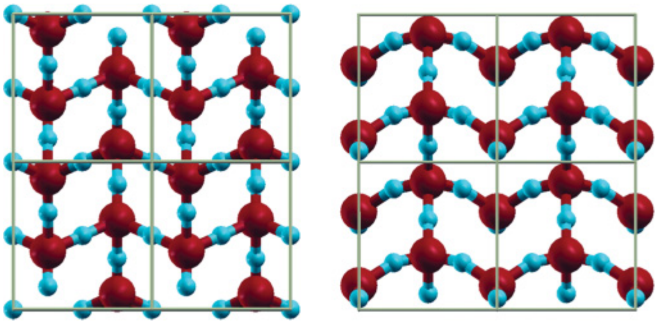

FIG. 2. (Color online) Ground-state structures of ice at 1 TPa. Left: *Pbcm*. Right: $Pmc2_1$.

Pbca was recently proposed as a likely candidate for the ground-state structure of ice from 760 GPa to 1.25 TPa.[14] However, Fig. 1 shows that it is only competitively stable with $Pmc2_1$ from ~800 to 925 GPa. It is certainly possible that *Pbca* is a stable phase of ice in this narrow pressure range. However, it is difficult to make this claim with certainty, as its lower enthalpy relative to *Pbcm* is within the tight convergence of the present calculations as well as the approximations employed (even though they are well justified—see Ref. 22). In any case, ~800 GPa marks a transition away from the symmetric hydrogen bonds seen in ice X and *Pbcm*, but which are again regained at much higher pressures (see below).

$Pmc2_1$ remains stable until ~1.3 TPa. It then becomes relatively unstable toward a structure with $P2_1$ symmetry, which is shown in Fig. 3. A comparison of Figs. 2 and 3 (left) shows that (in the plane of each figure) the O atoms

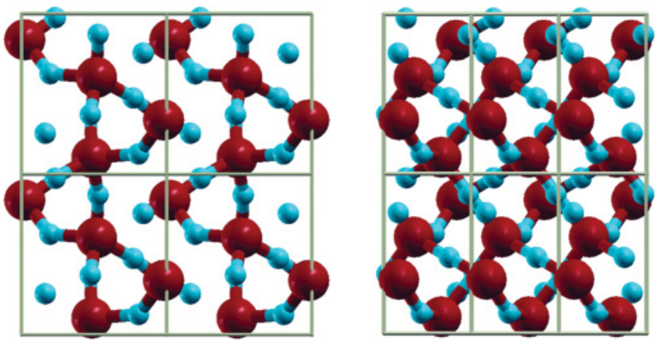

FIG. 3. (Color online) $P2_1$ at 1.4 TPa. Left: Same perspective as in Fig. 2. Right: Side view.

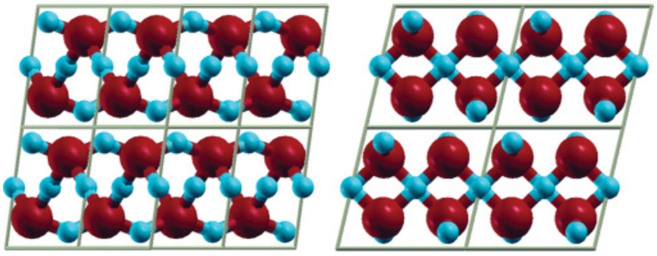

FIG. 4. (Color online) $C2/m$ at 5 TPa. The perspectives are similar to those shown in Fig. 3. Note that alternating O atoms are out of the plane relative to one another.

continue to remain close to their distorted hcp positions. Into the plane, however, $P2_1$ undergoes a noticeable compression and slight distortion relative to $Pbcm$ (not shown). Moreover, it can be seen that a further reorganization of the hydrogen-bond network occurs. O atoms in every other column (see above) continue to remain connected to their vertical neighbors, but the hydrogen bonds distort slightly outward in alternating directions. The hydrogen bonds of the other O atoms, on the other hand, rearrange more significantly. Each of these O atoms become connected to either one neighboring column or the other, also in an alternating fashion.

$P2_1$ remains the lowest-enthalpy structure up to the highest pressure considered in this work of 5 TPa. However, another competitive structure was also found in this pressure range, $C2/m$. Figure 1 shows that the relative enthalpy difference between $C2/m$ and $P2_1$ slowly decreases with increasing pressure. A linear extrapolation of the enthalpy versus pressure curves near 5 TPa (which should be quite accurate, given that both curves are nearly linear) indicates a transition pressure of ~5.29 TPa. As can be seen in Fig. 4, $C2/m$ is a layered structure, where each layer consists of two sets of O atoms. A slight shear deformation of the layers occurs, leaving the O atoms close to, but slightly displaced from their distorted hcp positions. Note that a slightly less stable structure without the shear deformation, $C2/c$, was also found (see below and Ref. 22). A comparison of the O atoms in Fig. 3 (right) with Fig. 4 (left) indicates that a transition toward the layered $C2/m$ structure is evident in $P2_1$ (and even $Pbcm$, which is similar, but less compressed, as discussed above). Moreover, symmetric hydrogen bonds are seen to be regained in $C2/m$, which connect the O atoms within each layer.

The sublattices of O atoms in all of the thermodynamically stable structures are similar to hcp. This packing first arises in the ice X → $Pbcm$ transition,[12] where the O atoms attempt to increase their packing efficiency (relative to bcc) to minimize the pV contribution to the enthalpy (where p and V are the pressure and volume, respectively). This is in contrast to the bcc-sublattice structures predicted in Ref. 14 (e.g., $Cmcm$), which explains their much lower enthalpies. At finite temperature, however, the O atoms again vibrate around bcc-sublattice positions (which is understandable, based on entropic considerations), and the protons become highly diffusive in a superionic phase.[27,28]

The results presented above were for static lattices. However, the light hydrogen mass causes the phases of ice at high pressures to have large zero-point energies (ZPEs) that must be estimated in order to determine the most stable ground-state structures. ZPEs were neglected during the AIRSS, but their impacts were estimated afterward using the harmonic approximation: $E_{\text{ZPE}} = \int d\omega F(\omega)\hbar\omega/2$, where $F(\omega)$ is the phonon density of states. $F(\omega)$ was calculated using a 2^3 grid of $\mathbf{q}$ points in the BZ, which is estimated to be sufficient to converge ZPE differences between structures to within a few percent.

TABLE I. Band gaps (in eV) of select structures of high-pressure ice.

Pressure (TPa)	$Pbcm$	$Pbca$	$Pmc2_1$	$P2_1$
0.4	9.63			
0.6	8.96			
0.8	8.66	8.45	7.16	
1.0	8.49	7.27	6.67	
1.2			6.27	5.92
1.4			5.93	5.76
1.6			5.63	5.54
2.0				5.16
3.0				4.34
4.0				3.64
5.0				3.03

Reference 22 shows that the ZPEs are quite large, increasing from 0.917 eV/H_2O at 400 GPa to 1.726 eV/H_2O at 5 TPa. Despite such large values, ZPE differences between the structures are relatively small, in all cases within 0.03 eV/H_2O. While this energy scale is not enough to change the enthalpic ordering of the structures, it is enough to affect precise transition pressures, in some cases. For example, $P2_1$ is found to have a lower ZPE than both $Pmc2_1$ and $C2/m$, causing the corresponding transition pressures to be shifted to 1.17 and 5.62 TPa, respectively. The ZPE difference between $Pbcm$ and $Pmc2_1$, on the other hand, is found to be practically negligible, resulting in a shift of the transition pressure higher by less than 50 GPa. Note that these estimates neglect the impact of zero-point pressures, which, given the small differences in ZPE between the structures, should have even less of an effect.

One of the most intriguing predictions regarding high-pressure ice is its metallization.[13] $Pbcm$, $Pmc2_1$, and $P2_1$ were all found to be wide band-gap insulators; see Table I. Furthermore, band-gap closure in these structures was found to occur very slowly with increasing pressure. However, $C2/m$ was metallic at all pressures considered. Metallization in $C2/m$ is seen to arise from the slight shear deformation of the O atoms, as the nearly identical $C2/c$ structure without this deformation remains insulating even at 5 TPa with a band gap of 0.96 eV. (See Ref. 22 for a discussion of the electronic band-structure of $C2/m$.) The $P2_1 \rightarrow C2/m$ transformation at 5.62 TPa therefore marks the insulator-to-metal transition in ice. This metallization pathway (as opposed to pressure-induced band-gap closure) is similar to that predicted in Ref. 14 at 1.55 TPa (by a transition to the metallic $Cmcm$ structure), but occurs at a significantly higher pressure, due to the large stability range of the insulating $P2_1$ structure.

The predicted insulator-to-metal transition in ice occurs at a pressure (5.62 TPa) similar to that in the superionic phase at finite temperature.[29] In the latter case, metallization coincides with a shift of the H atoms from symmetric to octahedral sites. Given that the underlying sublattice of O atoms does not change (which is responsible for the metallization in $C2/m$), it is likely that the metallization pathway in this case is more closely related to a pressure-induced band-gap closure than due to a transition to a naturally metallic state. Metallization by the former pathway is thus seen to occur at a lower pressure than it would in one of the analogous ground-state structures (e.g., $Pbcm$, $Pmc2_1$, or $P2_1$), consistent with typical finite-temperature behavior.

In conclusion, AIRSS was used to predict the ground-state and (zero-temperature) metastable structures of ice at high pressures. The predicted transformation sequence is ice X (Ref. 9) → $Pbcm$ (300−400 GPa) (Ref. 12) → $Pmc2_1$ (800−950 GPa) → $P2_1$ (1.17 TPa) → $C2/m$ (5.62 TPa), where transition pressures have been indicated in parentheses. The previously predicted $Pbca$ structure[14] was also found near 800–925 GPa. However, the relative stabilities between $Pbcm$, $Pbca$, and $Pmc2_1$ in this narrow pressure range were found to be indistinguishable within the convergence of the calculations. The $P2_1 \rightarrow C2/m$ transformation was demonstrated to mark the insulator-to-metal transition in ice, which is beyond pressures found inside even many giant planets, such as Jupiter. It can therefore be concluded that the (water) ice components in them remain insulating. There is, of course, the caveat that at planetary pressures, the corresponding temperatures are often very high as well.[3] This could result in the melting of ice to liquid water, and work is currently underway to determine the associated temperatures where this occurs. Nonetheless, along with the recent work elucidating the high-temperature phase diagram of water at high-pressure,[28] the results presented herein provide a relatively comprehensive picture of the high-pressure phase diagram of H_2O.

Note added. Recently, predictions of some of these structures were made via different methodologies in Refs. 30 and 31.

J.M.M. was supported by DOE DE-FC02-06ER25794 and DE-FG52-09NA29456. This research was also supported in part by the National Science Foundation through TeraGrid resources provided by NICS under Grant No. TG-MCA93S030.

---

[*] mcmahonj@illinois.edu

[1] P. V. Hobbs, *Ice Physics* (Oxford University Press, New York, 1974).

[2] W. B. Hubbard, *Planetary Interiors* (Van Norstrand Reinhold, New York, 1984).

[3] T. Guillot, Science **286**, 72 (1999).

[4] A. F. Goncharov, V. V. Struzhkin, M. S. Somayazulu, R. J. Hemley, and H. K. Mao, Science **273**, 218 (1996).

[5] K. K. M. Lee *et al.*, J. Chem. Phys. **125**, 014701 (2006).

[6] D. K. Bradley *et al.*, Phys. Rev. Lett. **102**, 075503 (2009).

[7] G. Malenkov, J. Phys. Condens. Matter **21**, 283101 (2009).

[8] C. G. Salzmann, P. G. Radaelli, E. Mayer, and J. L. Finney, Phys. Rev. Lett. **103**, 105701 (2009).

[9] A. Polian and M. Grimsditch, Phys. Rev. Lett. **52**, 1312 (1984).

[10] M. Benoit, A. H. Romero, and D. Marx, Phys. Rev. Lett. **89**, 145501 (2002).

[11] R. Caracas, Phys. Rev. Lett. **101**, 085502 (2008).

[12] M. Benoit, M. Bernasconi, P. Focher, and M. Parrinello, Phys. Rev. Lett. **76**, 2934 (1996).

[13] A. Polian, J. M. Besson, and M. Grimsditch, in *Solid State Physics Under Pressure*, edited by S. Minomura (Terra Scientific, Tokyo, 1985), pp. 93–98.

[14] B. Militzer and H. F. Wilson, Phys. Rev. Lett. **105**, 195701 (2010).

[15] C. J. Pickard and R. J. Needs, Phys. Rev. Lett. **97**, 045504 (2006).

[16] C. J. Pickard and R. J. Needs, J. Phys. Condens. Matter **23**, 053201 (2011).

[17] J. M. McMahon and D. M. Ceperley, Phys. Rev. Lett. **106**, 165302 (2011).

[18] P. Giannozzi *et al.*, J. Phys. Condens. Matter **21**, 395502 (2009), [http://www.quantum-espresso.org].

[19] N. Troullier and J. L. Martins, Phys. Rev. B **43**, 1993 (1991).

[20] P. H.-L. Sit and N. Marzari, J. Chem. Phys. **122**, 204510 (2005).

[21] J. P. Perdew, K. Burke, and M. Ernzerhof, Phys. Rev. Lett. **77**, 3865 (1996).

[22] See Supplemental Material at http://link.aps.org/supplemental/10.1103/PhysRevB.84.220104 for additional computational details and results.

[23] C. Lee, D. Vanderbilt, K. Laasonen, R. Car, and M. Parrinello, Phys. Rev. Lett. **69**, 462 (1992).

[24] P. E. Blöchl, O. Jepsen, and O. K. Andersen, Phys. Rev. B **49**, 16223 (1994).

[25] W. L. Mao, H.-k. Mao, Y. Meng, P. J. Eng, M. Y. Hu, P. Chow, Y. Q. Cai, J. Shu, and R. J. Hemley, Science **314**, 636 (2006).

[26] C. J. Pickard and R. J. Needs, J. Chem. Phys. **127**, 244503 (2007).

[27] C. Cavazzoni, G. L. Chiarotti, S. Scandolo, E. Tosatti, M. Bernasconi, and M. Parrinello, Science **283**, 44 (1999).

[28] M. French, T. R. Mattsson, N. Nettelmann, and R. Redmer, Phys. Rev. B **79**, 054107 (2009).

[29] M. French, T. R. Mattsson, and R. Redmer, Phys. Rev. B **82**, 174108 (2010).

[30] M. Ji, K. Umemoto, C.-Z. Wang, K.-M. Ho, and R. M. Wentzcovitch, Phys. Rev. B **84**, 220105 (2011).

[31] A. Hermann, N. W. Ashcroft, and R. Hoffmann (to be published).